Fabrication and characterization of three-dimensional nanofiber membrance of PCL–MWCNTs by electrospinning

Z.X. Meng [a], W. Zheng [a], L. Li [a], Y.F. Zheng [a,b,*]

[a] Center for Biomedical Materials and Engineering, Harbin Engineering University, Harbin 150001, China
[b] Department of Advanced Materials and Nanotechnology, College of Engineering, Peking University, Beijing 100871, China

ARTICLE INFO

ABSTRACT

The uniform and highly smooth nanofibers of poly(ε-caprolactone) (PCL) composited with different multi-walled carbon nanotubes (MWCNTs) content (ranging from 0.1 wt.% to 5 wt.%) were successfully prepared by electrospinning method without the occurrence of bead defects in this study. The PCL–0.5 wt.%MWCNTs nanofiber membrane exhibited the maximum tensile strength (about 1.42 MPa), which was increased by 46% compared with that of electrospun pure PCL nanofiber membrane. Moreover, the PCL–MWCNTs nanofiber membrane exhibited three-dimensional porous structure with a high porosity over 90%. The average diameter of PCL–MWCNTs nanofibers decreased with the addition of MWCNTs and there was a narrow diameter distribution in the range of 52–244 nm when the amount of MWCNTs was 0.5 wt.%. Compared with pure PCL nanofibers, PCL–MWCNTs nanofibers showed accelerating degradation behavior. In addition, the cytotoxicity results revealed that the electrospun PCL–MWCNTs nanofiber membranes possessed good in vitro biocompatibility, and hemolysis and kinetic clotting tests indicated that the PCL nanofiber membranes did not enhance blood coagulation after the addition of MWCNTs. It can be concluded that such kind of electrospun PCL–MWCNTs nanofibers may be promising candidate for tissue engineering scaffold application.

1. Introduction

Electrospinning is a simple method which can produce ultrafine fibers with diameters ranging from nanometer to micron scales through high electric field [1,2]. Comparing with other scaffolds, electrospun scaffold has high specific surface area, high porosity and the three-dimensional reticulate structure, which is similar to the natural extracellular matrix. Moreover, more pores interconnected to each other would accelerate metabolism of the cells [3]. Therefore, the electrospun nanofibers membrane can be used as tissue engineering scaffold [4], wound dressing articles [5], artificial blood vessels [6] and drug delivery [7] in biomedical field and has received increasing attentions in the past few years.

Poly(ε-caprolactone) (PCL) is an FDA-approved biodegradable polymer with excellent biocompatibility and flexibility, which has attracted increasing interest in many areas such as biodegradable packaging materials, implantable biomaterials and microparticles for drug delivery [8]. However, several disadvantages of PCL were also recognized, for example, (i) it degraded much slower than other

known biodegradable polymers, which restricted their practical application range; (ii) the mechanical properties of the PCL scaffolds with high porosity were poor, which limited their use in hard tissue engineering. To overcome these shortcomings, PCL based composite such as the PCL/collagen [9], PCL/gelatin [10] and PCL/nanoAgZ electrospinning nanofibers composite membrane [11] were widely investigated.

Nanomaterials usually exhibit special properties and potential applications, therefore they have attracted considerable research attention in the recent ten years [12,13]. Carbon nanotubes (CNT), since their discovery in 1991, have captured the imagination of scientists worldwide and been the focus of numerous investigations due to their unique structural, mechanical, physical and chemical properties [14,15]. With synthesis technology and purification method of the CNTs being gradually matured, more attentions have been focused on the application of the CNTs. One of the most promising applications of CNTs is the fabrication of polymer/CNTs nanocomposite to improve the mechanical and electrical properties of the polymer matrix [16–19]. The techniques for polymer/CNTs nanocomposite fabrication include solution casting [20], melt processing [21] and electrospinning [22,23].

In this study, we employed the electrospinning method to prepare PCL–MWCNTs nanofiber with different MWCNTs content (ranging from 0.1 wt.% to 5 wt.%), with the aims to investigate the effect of MWCNTs content on (i) mechanical properties of composite membranes; (ii)

* Corresponding author. Postal address: Department of Advanced Materials and Nanotechnology, College of Engineering, Peking University, No.5 Yi-He-Yuan Road, Hai-Dian District, Beijing 100871, China. Tel./fax: +86 451 82518644.
E-mail address: yfzheng@pku.edu.cn (Y.F. Zheng).

physical and chemical properties of composite membranes; and (iii) biocompatibility and hemocompability of composite membranes.

2. Materials and methods

2.1. Materials

Poly(ε-caprolactone) (PCL; M_w ~ 100,000) was purchased from Jinan Daigang Biomaterial Co. Ltd. (China). Multi-walled nanotubes (MWCNTs, diameter 10–30 nm, length 1–2 μm with a purity of >97%) were purchased from Shenzhen Nanotech Port Co., Ltd (Shenzhen, China). The MWCNTs samples were purified by refluxing the as-received MWCNTs in 3:1 (v/v) mixture of concentrated H_2SO_4 (98 wt.%)/HNO_3 (60 wt.%) for 5 h and prior to use. Dichloromethane and methanol, used as the solvent, were purchased from Tianjin Chemical Reagents Company (China). All the other chemicals were of analytical reagent grade and used without further purification.

2.2. Electrospinning of PCL–MWCNTs nanofibers

The PCL–MWCNTs composite nanofiber membrane studied in the present study was produced by electrospinning. Firstly, the MWCNTs were dispersed in dichloromethane/methanol solution (3:1 v/v) and the mixture was sonicated for 1 h to obtain a homogeneous and black dispersion with various concentrations. To this dispersion, 10 wt.% PCL solution in a solvent mixture of dichloromethane and methanol (3:1 v/v) was added dropwise with ultrasonic stirring. The final concentrations of MWCNTs were 0.1%, 0.5%, 1%, 2% and 5% with reference to PCL mass in the mixture, respectively.

For electrospinning, 5 mL of each kind of PCL–MWCNTs solution was loaded in a syringe and injected through a stainless-steel blunt-ended needle at an injection rate of 0.5 mL/h using an infusion pump (TS2-60, Baoding Longer Precision Pump Co., China) between the metal collector and the needle tip of 10 cm under a driving voltage of 10 kV by high voltage power supply (HB-F303-1AC, China). All electrospinning processes were performed at ambient temperature (18 ± 2 °C).

2.3. Characterizations of the electrospinning membranes

The morphologies of the electrospun PCL–MWCNTs nanofiber membrane before and after degradation were observed by scanning electron microscope (CamScan MX2600FE, UK) at an accelerating voltage of 15 kV. All samples were coated with a thin layer of palladium in two 30 s consecutive cycles at 45 mA to reduce charging and produce a conductive surface. The diameters of resulting nanofibers were analyzed using software Image J.

The apparent density of each experimental electrospun membrane was determined by an average of three samples using density bottle methods. The porosity of electrospinning nanofibrous membrane was calculated by using the following equation [6].

$$Porosity(\%) = (1 - \rho / \rho_0) \times 100\%$$

Where ρ is the density of the electrospinning membrane, ρ_0 is the density of the bulk polymer.

X-ray diffraction analysis was characterized by X-ray diffractometer (FEI Company, USA) equipped with Cu-Kα source and operating at 40 kV and 40 mA. The diffraction patterns were obtained at a scan rate of 5°/min.

The thermal properties of all electrospinning membrane were investigated by the differential scanning calorimetry (DSC) measurements (Perkin-Elmer Company, USA) in a temperature range from −80 °C to 80 °C at a heating rate of 10 °C/min under a nitrogen atmosphere. Samples with a weight of approximately 5 mg were loaded in a aluminum crucible under dry condition. The degree of

crystallinity (X_c) of the PCL in the nanofibrous membrane was calculated by the following formula:

$$X_c(\%) = \Delta H_m / \Delta H_m^* \times 100\%$$

where ΔH_m^* is 139 J/g, which is the theoretical heat of fusion for 100% crystalline PCL [24].

Tensile tests of the electrospinning nanofibrous membrane were carried out with a BOSE ElectroForce 3200 test instruments by applying a 225 N load cell at a crosshead speed of 0.5 mm/min. All samples were cut into rectangle with dimensions of 20 × 5 mm² and horizontally mounted on two mechanical gripping units of the tester, leaving a 10 mm gauge length for mechanical loading. The sample thicknesses were measured with a micrometer having a precision of 1 μm. The average values for the tensile property were obtained from the results of three tests.

The electrospinning PCL–MWCNTs nanofiber membranes were placed at 37 °C in closed bottles containing 7 mL of phosphate buffer solution (pH 7.4) for up to 8 weeks. The incubation medium was replaced once per week. At given time intervals, the electrospinning PCL–MWCNTs nanofiber membranes were taken out and washed with deionised water, dried under vacuum for 48 h to remove the solution completely. Degradation was evaluated by the weight loss (%) according to the following equation:

$$Weight\, loss(\%) = (W_0 - W_t) / W_0 \times 100\%$$

Where W_0 is the weight of each sample before submersion in the buffer solution, W_t is the weight of the sample after submersion in the buffer solution for specified time points in its dry state. An average of three measurements was taken for each group.

2.4. Cytotoxicity evaluation

In this study, mouse fibroblast cells (L-929 and NIH3T3) were used to assess the cytotoxicity of the PCL–MWCNTs nanofiber membranes by the addition of their extracts to a cell culture on a 96-multiwell plate, 1.0 g each sample, sterilized by UV irradiation, individually poured into 15-mL glass flasks with 10 mL DMEM. The flasks were simultaneously incubated in a humidified atmosphere with 5% CO_2 at 37 °C for 72 h. Then, the supernatant fluid was centrifuged to prepare the extraction medium, and then refrigerated at 4 °C before the cytotoxicity test. L-929 and NIH3T3 were cultured in Dulbecco's modified Eagle's medium (DMEM), supplemented with 10% fetal bovine serum (FBS), 100 U/mL penicillin and 100 μg/mL streptomycin in humidified incubator at 37 °C with 5% CO_2. When cell reached 80–90% confluence, they were trypsinized and counted with a hemocytometer. The cells were added to each well of a 96-well tissue culture plate at a density of 1×10^5 cells/mL in 100 μL medium per well. After 24 h culture, the medium was replaced with 100 μL negative control (DMEM), positive control (DMEM with 10% (v/v) dimethylsulfoxide) and experimental material extraction groups, respectively, and the cells were cultured in a humidified atmosphere with 5% CO_2 at 37 °C up to desired time points. At desired time points, the cells were incubated in 10 mL MTT (10 mg/mL) for 4 h in 5% CO_2 incubator at 37 °C. Then 100 ml sodium dodecyl sulfate (10 wt.% SDS in 0.01 M HCl) was added in each well and incubated for day and night to dissolve the internalized purple formazan crystals. The absorbance was measured at 570 nm with a reference wavelength of 630 nm by microplate reader (Bio-RAD680, Bio-rad Co., USA). The relative growth rate (RGR) was calculated by the following equation:

$$RGR(\%) = D_t / D_{nc} \times 100\%$$

Where D_t is the absorbance of the test samples, D_{nc} is the absorbance of the negative reference.

2.5. Hemocompatibility

In the hemolysis test, blood was drawn from healthy adult volunteers by venipuncture into acid citrate dextrose (ACD) anticoagulant vacutainer tubes and then diluted with 0.9% saline. The PCL–MWCNTs nanofiber membranes (10×10 mm² in area) were washed with distilled water two times and then put into a test tube with 10 mL 0.9% saline and incubated for 30 min at 37 °C. After that, 0.2 mL of diluted blood was added into test tube and incubated for 60 min at 37 °C. Similarly, 0.2 mL of diluted blood was added to 10 mL of distilled water and 0.9% saline solution using as a positive and negative controls, respectively. After the incubation, all the samples were centrifuged at 3000 rpm for 5 min. Then the supernate was determined for the absorbance at 540 nm using a spectrophotometer (UV-2550, Japane). The hemolysis percentage (HP) can be calculated by the following equation:

$$HP(\%) = (D_t - D_{nc}) / (D_{pc} - D_{nc}) \times 100\%$$

Where D_t is the absorbance of the test samples; D_{pc} and D_{nc} are the absorbance of the positive and negative control, respectively. The hemolysis results were average of three measurements.

The anticoagulant properties of the PCL–MWCNTs nanofiber membranes were evaluated by the kinetic clotting time method [25]. A 0.2 mL of ACD blood was dropped on the surface of the samples and glass coverslips, followed by addition of 50 μL of CaCl₂ (0.2 mol/L) solution and mixed uniformly. After a predetermined period of time (5, 10, 20, 30, 40 and 50 min), the specimens were put into 50 mL distilled water and incubated for 5 min. The concentration of free hemoglobin in water was colorimetrically measured by monitoring the absorbance at 540 nm using spectrophotometer.

2.6. Statistical analysis

The data was expressed as means ± standard deviation (SD) and was analyzed by SPSS11.0. Differences were considered statistically significant at $p < 0.05$.

3. Results and discussion

3.1. Microstructural characterization of electrospun PCL–MWCNTs nanofiber membranes

Fig. 1 shows the SEM micrographs of PCL–MWCNTs nanofiber membranes containing different MWCNTs ranging from 0 wt.% to 5 wt.%. As can be seen from Fig. 1, uniform and highly smooth nanofibers were formed without the occurrence of bead defects for all experimental materials. Among them, the electrospun pure PCL nanofibers had an average fiber diameter of 230 ± 100 nm (Table 1). It can be seen that the electrospun PCL–0.5 wt.%MWCNTs nanofiber diameter was smaller than that of the electrospun PCL nanofibers with a narrow diameter ranging from 52 nm to 244 nm. However, further increase of the MWCNTs content led to the increase of average diameter of PCL–MWCNTs nanofibers with broader diameter distribution. For electrospinning, solution electrical conductivity is an important factor that influences the fiber diameter and distribution. Under the electrostatic field, the droplet of polymer solution at the nozzle connected to electrical pole would deform into a Taylor conical shape and charge or dipole orientation would be formed at the interface between air and droplet to form tensile force. Once the tensile force overcame the surface tension of droplet, a jet of solution would eject from droplet and underwent a process of stretching, splitting and whipping in the air and finally changed into fiber when the solvent evaporated from the jet. Therefore, polymer solution with higher electrical conductivity would carry more charge leading to

greater tensile force which might increase stretching and splitting of the jet, resulting in thinner fiber and broader diameter distribution. However, if the solution flow was enough, thicker jet would eject by greater tensile force which led to thicker fiber diameter [26]. In this paper, since the addition of MWCNTs could increase electrical conductivity of polymer solution and solution flow was enough, a lower filler of MWCNTs would result in thinner fiber, and further increase of MWCNTs led to thicker fiber diameter with broader fiber distribution, which were the synthetical results influenced by the two factors. Compared with the F-MWCNT/PCL and P-MWCNT/PCL nanofibers reported by Saeed et al. [23], in this study both the average fiber diameter and the diameter distribution of PCL–MWCNTs nanofibers were smaller. More importantly, in previous reports many beads (more than 1 μm) appeared along the MWCNT/PCL fibers with increasing the amounts of MWCNTs, and the MWCNTs/PCL composites contained more than 2 wt.% of MWCNTs were not able to be electrospun into fibers. Yet in this study there was no formation of the bead, and the PCL–5 wt.%MWCNTs composites were still able to be successfully electrospun into nanofibers. The reason might be that the present nanocomposite solution with noncovalently functionalized MWCNTs possessed excellent conductivity and elasticity [27]. At the same time, for all the electrospun membranes, PCL–MWCNTs nanofiber can be deposited in a convoluted three-dimensional porous manner with a high porosity up to 90% (as listed in Table 1), which is beneficial for adherence and proliferation of cells.

Fig. 2 shows the XRD patterns for bulk PCL and various PCL–MWCNTs nanofiber membrane samples. As can be seen in all cases, two strong diffraction peaks at Bragg angles $2\theta = 21.4°$ and $23.8°$ could be observed, which was attributed to the diffraction of the (110) lattice plane and the (200) lattice plane of semi-crystalline PCL, respectively [28]. However, compared with the pure PCL nanofiber membrane, the intensity of two diffraction peaks for PCL–MWCNTs nanofiber membrane was significantly decreased, which might due to that the electrospun process would retard the crystallization of PCL. Moreover, with the increase of MWCNTs content, the diffraction intensity was firstly increased and then decreased, which has a maximum at 1 wt.% MWCNTs content. There results were similar to those of other polymer matrix composite containing MWCNTs previously reported [29,30]. It has been shown, for example, that the PVDF/MWCNTs composites with high aspect ratio of MWCNTs have the β phase structure for MWCNTs loading level equal to 2 wt.%, whereas the composites with low aspect ratios of MWCNTs always have a mixture of α and β phases for MWCNTs concentration less than 2 wt.% [30]. Therefore, from these results it was concluded that the content of MWCNTs can not only influence the crystallization but also the crystal type of PCL.

The thermal and crystalline properties of bulk PCL and electrospun PCL–MWCNTs nanofiber membranes analyzed by DSC were listed in the Table 2. It can be seen that the melting temperature (T_m) and the crystallization of bulk PCL film were higher than that of porous electrospun PCL nanofiber membrane. This result was very consistent with that of XRD result. In addition, with the increase of MWCNTs content, the crystallization of PCL–MWCNTs nanofiber membrane samples increased a little and had a maximum at 1 wt.% MWCNTs content. Subsequently, with the concentration of MWCNTs increased further to 5 wt.%, the crystallization of PCL–MWCNTs nanofiber membrane sample, however, was decreased. The reason might be the enhancement of nucleation ability by the well-dispersed individual MWCNTs [31,32].

3.2. Mechanical properties of electrospun PCL–MWCNTs nanofiber membranes

Fig. 3 shows the typical tensile stress–strain curves for electrospun nanofiber membranes. As can be seen from Fig. 3, at the lower MWCNTs filler content, the tensile strength of PCL–MWCNTs nanofiber membranes increased with increasing MWCNTs filling content (0.1 and
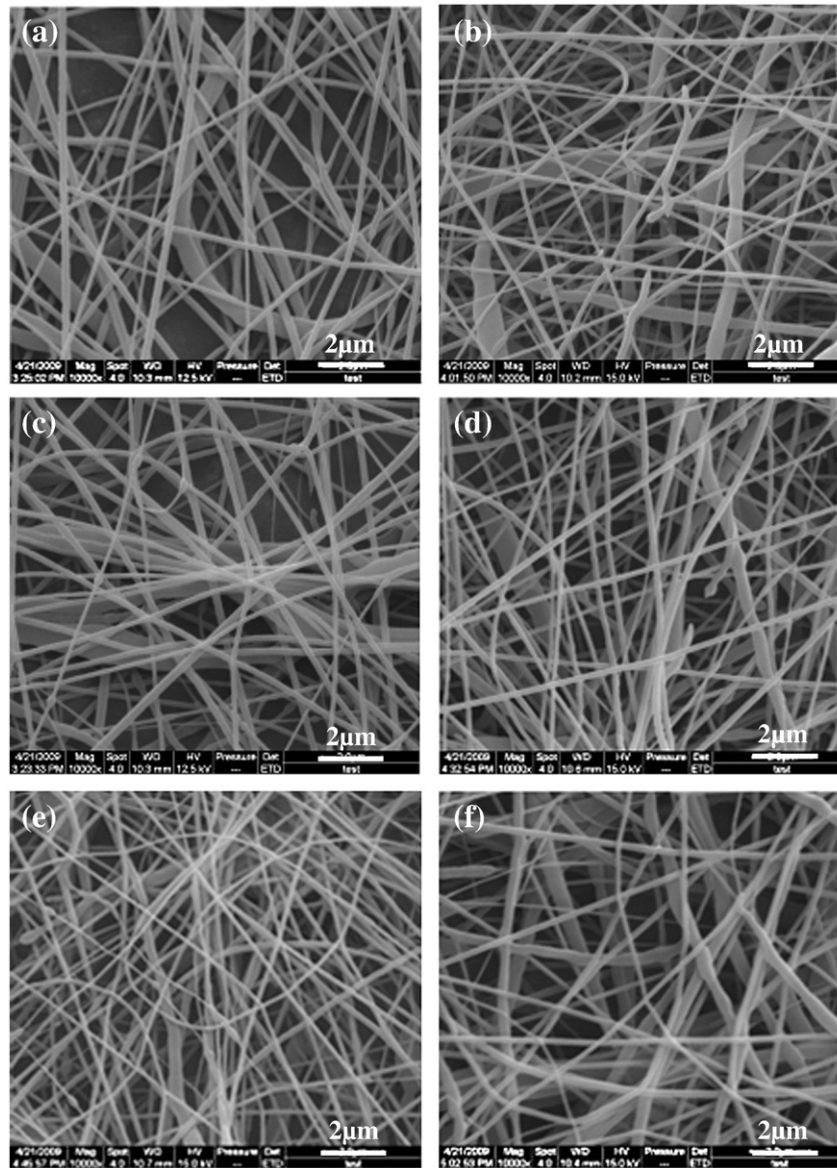
Fig. 1. SEM image of electrospun (a) pure PCL, (b) PCL–0.1 wt.%MWCNTs, (c) PCL–0.5 wt.%MWCNTs, (d) PCL–1 wt.%MWCNTs, (e) PCL–2 wt.%MWCNTs and (f) PCL–5 wt.%MWCNTs nanofiber membranes.

0.5 wt.%). Subsequently, further increasing the filler content (1, 2 and 5 wt.%) lead to the decrease of tensile strength of PCL–MWCNTs nanofiber membranes. Moreover, the PCL–0.5 wt.%MWCNTs sample exhibited the maximum strength (about 1.42 MPa). In addition, the PCL–0.1 wt.%MWCNTs and PCL–0.5 wt.%MWCNTs nanofiber membranes showed higher tensile strength compared with pure PCL nanofiber membrane. As is well-known, nanomaterials have high surface energy and are easy to aggregate, which lead to the poor

Table 1
Fiber diameter, density and porosity of electrospun PCL and PCL–MWCNTs nanofiber membranes.

Samples	Average diameter (nm)	Diameter distribution (nm)	Porosity (%)
Pure PCL	230 ± 100	100–482	92.14
PCL–0.1 wt.%MWCNT	207 ± 72	89–403	91.19
PCL–0.5 wt.%MWCNT	117 ± 45	52–244	91.92
PCL–1 wt.%MWCNT	203 ± 79	91–479	91.43
PCL–2 wt.%MWCNT	221 ± 104	102–548	92.58
PCL–5 wt.%MWCNT	252 ± 146	141–860	90.32
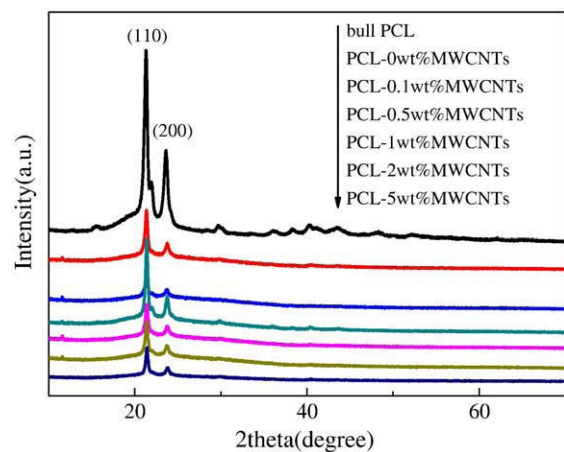
Fig. 2. XRD patterns of purified MWCNTs, PCL film, and electrospun PCL–MWCNTs nanofiber membranes.
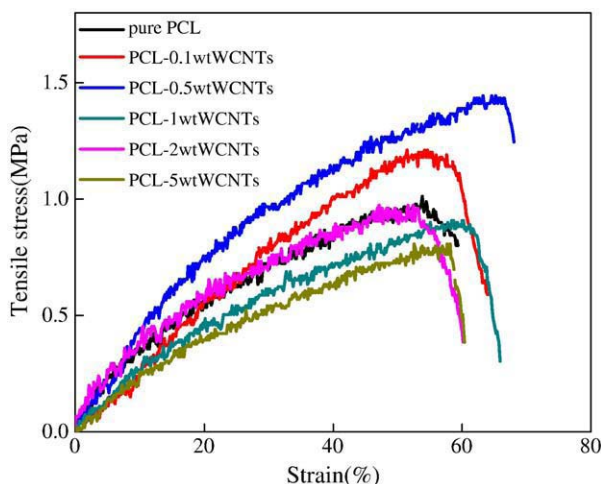
Table 2
Thermal and crystalline properties of bulk PCL and electrospun PCL–MWCNTs nanofiber membranes.

| Samples	T_m (°C)	ΔH_m (J/g)	X_c (%)
Bulk PCL	66.50	67.73	47.69
PCL–0 wt.%MWCNTs	58.39	53.92	37.98
PCL–0.1 wt.%MWCNTs	57.61	55.36	38.99
PCL–0.5 wt.%MWCNTs	56.93	55.48	39.07
PCL–1 wt.%MWCNTs	56.76	64.75	45.60
PCL–2 wt.%MWCNTs	56.59	60.24	42.42
PCL–5 wt.%MWCNTs	56.26	52.55	37.01

dispersion of nanomaterials in polymer matrix. Thus, good dispersion of CNTs in a polymer matrix provided more uniform stress distribution, minimized the presence of stress-concentration centers, and increased the interfacial area for stress transfer from the polymer matrix to the CNTs [33]. On the other hand, in addition to the individual fiber properties, the interaction between fibers in the fibrous mats contributed to the mechanical properties of the mats [34]. The PCL–0.5 wt.% MWCNTs nanofibers showed the finest fiber sizes (Table 2) and many nanofibers form membranes providing more contacts and thus stronger cohesion among fibers. These results indicated that nanocomposite fibers with less agglomeration and finest fiber sizes would produce fibers with better mechanical properties. Moreover, it was obvious that the yield point of the samples had irregularities. This may due to the fact that the nanofibers were randomly oriented distribution in the membrane. When the membrane was uniaxially stretched, only fibers along the elongation direction were stretched, and fibers of other direction generally slid and turned to the elongation direction and then stretched during the process of stretching. Thus the macro tensile behavior of the membrane was the total of a series of fibers stretching and sliding during different time, which led to irregular yield point of the samples.

3.3. Degradation behaviour of electrospun PCL–MWCNTs nanofiber membranes

For tissue engineering scaffold, biodegradable polymer attracts more attention because the high molecular weight chains would be hydrolyzed into oligomers which are non-toxic to human body. Degradation of PCL occurs by hydroxylation and fragmentation of high molecular weight chains, followed by changing to CO_2 and water in the environment of water or body fluid with or without enzyme. The degradation of PCL–MWCNTs nanofiber membranes was examined in vitro as showed in Fig. 4. It is well known that bulk PCL is widely used

Fig. 3. Typical tensile stress–strain curves of pure PCL and PCL–MWCNTs nanofiber membranes.
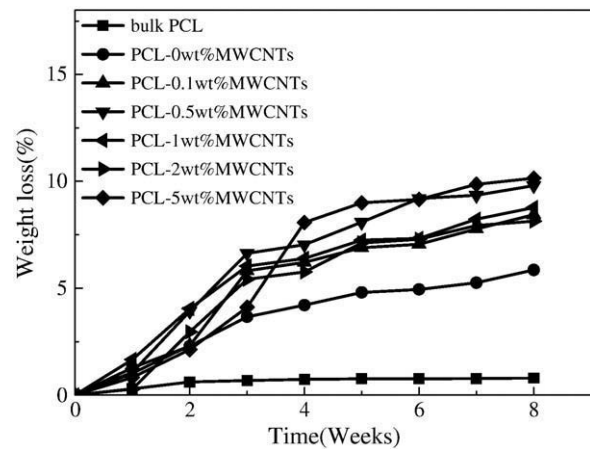
Fig. 4. In vitro degradation of pure bulk PCL and electrospun PCL–MWCNTs nanofiber membrane in PBS (pH 7.4) at 37 °C.

as long term implantable devices because of their slow degradation rates as compared to that of polylactide [35]. As can be seen from Fig. 4, the electrospun PCL–MWCNT nanofiber membranes with different MWCNTs content ranging from 0 wt.% to 5 wt.% showed an accelerating weight loss behavior when compared with the pristine bulk PCL which showed very small weigh loss (about 0.78%) after 8 weeks immersion. The main reason is that the crystallization of pristine bulk PCL was higher than that of electrospun PCL–MWCNTs nanofiber membranes. In general, in an aqueous environment, amorphous polymer degrades more readily than crystalline polymers [36]. On the other hand, in addition to the case of PCL–5 wt.%MWCNTs nanofiber membranes, the weight loss of PCL–MWCNTs nanofiber membranes were comparatively fast at initial three weeks compared with electrospun pure PCL nanofiber membranes and then increased reposefully. The effect of MWCNTs filling content on biodegradation behavior of PCL–MWCNTs nanofiber membranes was not obvious.

The morphological changes of the PCL–MWCNTs nanofiber membranes after degradation for 4 and 8 weeks in PBS were showed in Fig. 5. After 4 weeks of degradation, for the PCL–MWNTs nanofiber specimens, both fibrous and pore structures remained and a little part of fibers was chapped. Moreover, as can be seen in all cases, compared with initial state before degradation (Fig. 1), the diameter of nanofibers was apparently larger and it showed rough surface. After 8 weeks of degradation, the long PCL–MWCNT nanofibers degrade into sectioned short fibers and, eventually, decompose into powders. This was because at initial degradation, some low polymers hydrolyzed and diffused from the fibers, which resulted in more loose structure of the fiber and made water molecules diffuse into the fiber more easily. And with the time increasing, the long chains of polymer hydrolyzed and ruptured, which made the fibers break into pieces.

3.4. Cytotoxicity of electrospun PCL–MWCNTs nanofiber membranes

As a novel form of carbon, CNTs are expected to be most promising materials for biomedical applications, such as biosensors for detection of biomolecules and biological cells, disease diagnostics and drug delivery vehicles due to their unique structural, electrical, and mechanical properties. Therefore, the cytotoxicity of CNTs has attracted considerable research attention in the recent years [37–41]. However, the toxicity of CNTs is still controversial [40,41]. Here, the cytotoxicity test was carried out to investigate the biocompatibility of the PCL–MWCNTs nanofiber membranes using MTT assay for 3 days as shown in Fig. 6. It can be seen that L929 and NIH3T3 cells for the PCL–MWCNTs nanofiber groups were increasing in quantity and exhibited no significant differences in comparison with negative controls ($p < 0.05$), which indicated that the extracts of PCL–MWCNTs nanofibers were favorable
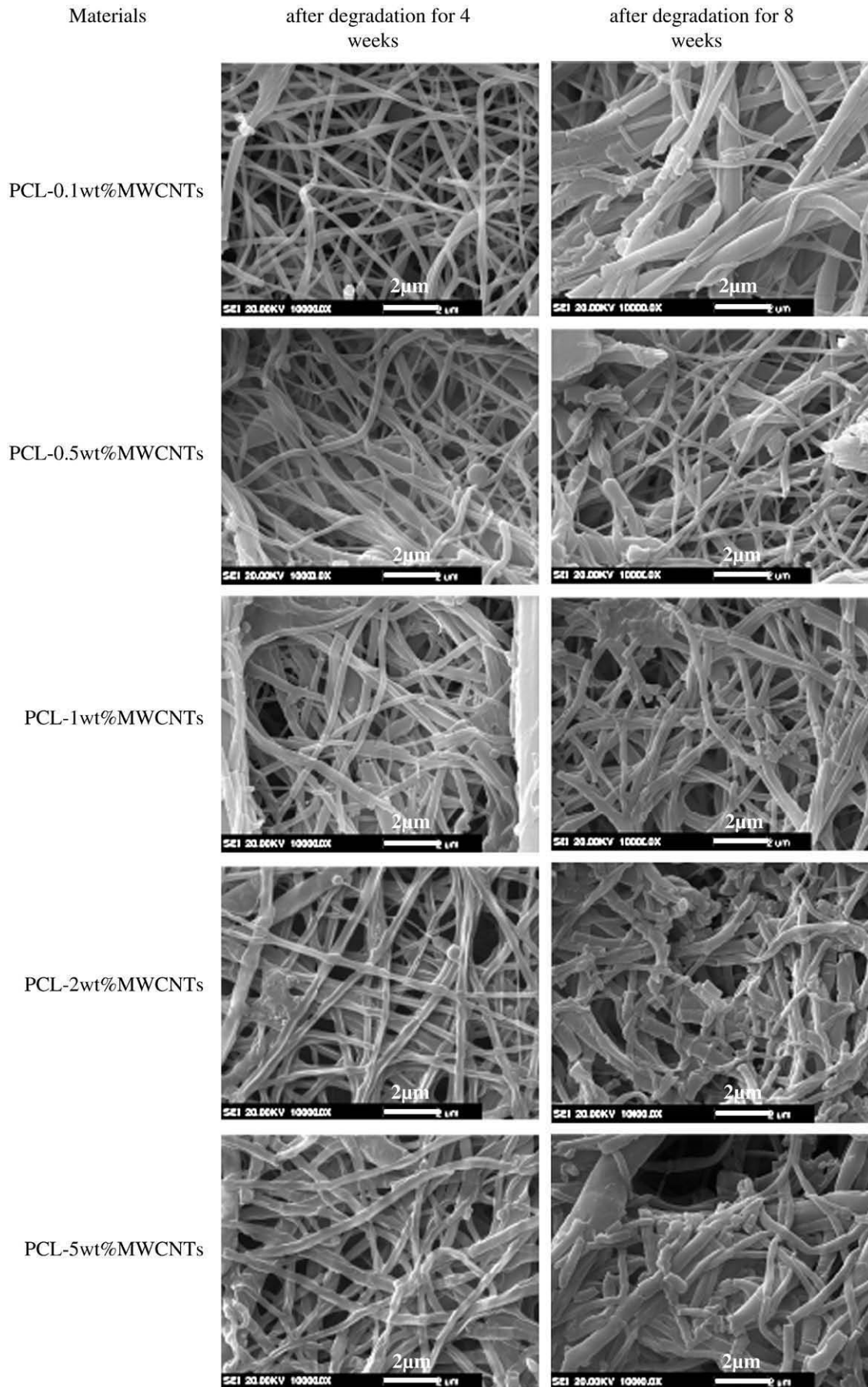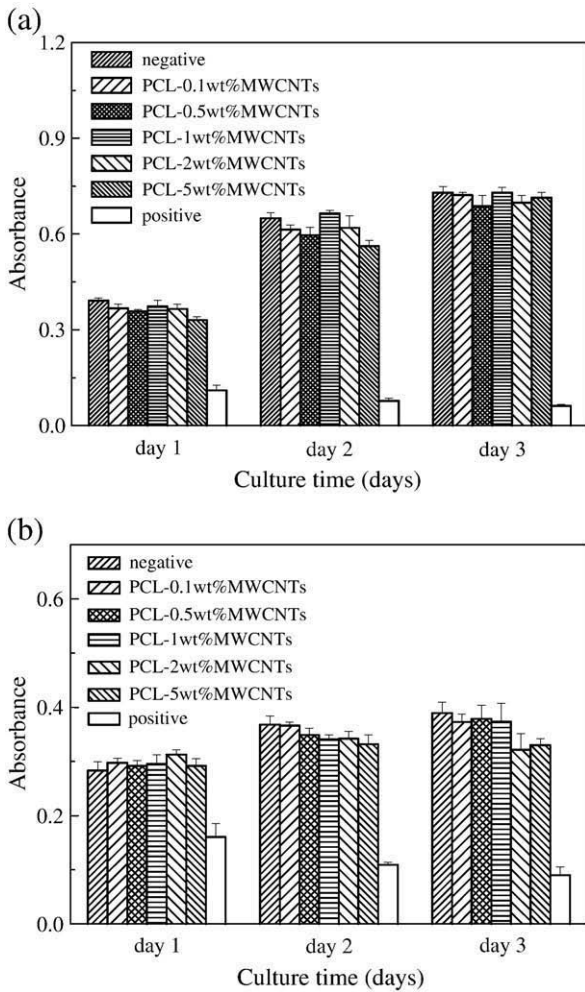
Materials	after degradation for 4 weeks	after degradation for 8 weeks
PCL-0.1wt%MWCNTs		
PCL-0.5wt%MWCNTs		
PCL-1wt%MWCNTs		
PCL-2wt%MWCNTs		
PCL-5wt%MWCNTs		

Fig. 5. Morphology of electrospun PCL–MWCNTs nanofiber membrane after degradation for 4 and 8 weeks.

(a)

(b)

Fig. 6. MTT assay of the L-929 (a) and NIH3T3 (b) cell proliferation after the cell was treated with extracts of electrospun PCL–MWCNTs nanofiber membranes. All values are means ± SD, n = 5.

to the adherence and proliferation of cells. Moreover, the extracts of the PCL–MWCNTs nanofibers with different content MWCNTs exhibited no or low cytotoxicity with a score of 0 or 1 grade according to the six-grade criteria of the Implante-GB/T 16175-1996 [42]. From the results given above, it might be concluded that the PCL–MWCNTs nanofiber membranes used in this study showed no cytotoxic effect due to added MWCNTs.

3.5. Hemocompatibility of electrospun PCL–MWCNTs nanofiber membranes

When the polymer contact with the tissue from a living body, it will lead to a number of important reactions, such as thrombosis. Thus, biocompatibility, especially blood compatibility, is the most important property with regard to biomedical materials. In this research work, the hemocompatibility of PCL–MWCNTs nanofiber membranes were evaluated by hemolysis and kinetic clotting time method. The hemolysis percentage (HP) represents the extent of red blood cells broken by the sample in contact with blood. Fig. 7 shows the HP of ACD blood with PCL–MWCNTs nanofibers membrane. From Fig. 7 it can be seen that the HP was less than 5% for all PCL–MWCNTs nanofiber membranes, indicating good character of anti-hemolysis among all the PCL–MWCNTs nanofiber membranes [43]. However, when the MWCNTs content reached 1 wt.%, the maximum HP of PCL–1 wt.%MWCNTs nanofiber membrane were 1.44 ± 0.63. Further increasing the MWCNTs content lead to the reduction of HP, which was probably because the surface roughness of
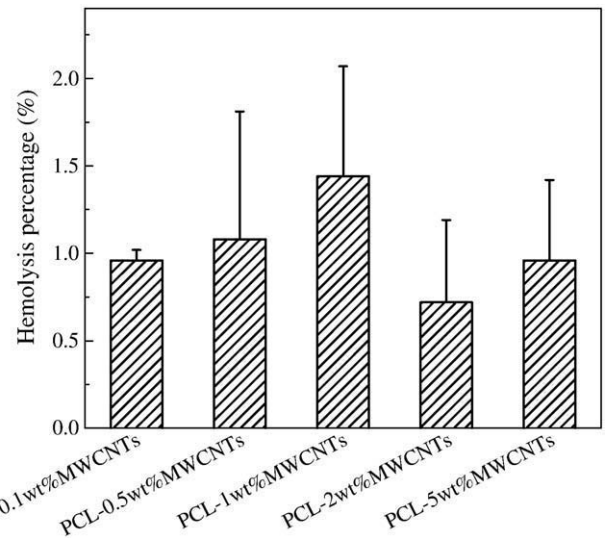

Fig. 7. Hemolysis percentage of electrospun PCL–MWCNTs electrospun nanofiber membranes.

PCL–MWCNTs nanofiber membranes increased as the MWCNTs concentration increased, so a shear stress lead to the red blood cells rupture and resulting in hemolysis when blood contact with rough surface of materials.

The blood clotting behavior of PCL–MWCNTs nanofiber membranes was shown in Fig. 8. The aim of in vitro dynamic clotting time test was to measure the activation extent of coagulation factor and the clotting time influenced by the material. The longer the clotting time was, the better anticoagulation the material possessed. From Fig. 8 it may be seen that the blood incubated with PCL–MWCNTs nanofiber membranes had a significantly higher absorbance than glass at each time point measured. Moreover, there was no significant difference in the degree of clotting until 50 min with the increasing concentration of MWCNTs. However, at 50 min time period for blood incubated with glass, the absorbance was only 0.103. These results showed that the PCL–MWCNTs nanofiber membranes have good anticoagulant property.

4. Conclusions

The PCL–MWCNTs nanofiber membranes were successfully produced without the occurrence of bead defects using electrospinning process. The fabricated PCL–MWCNTs nanofiber membranes possessed high porosity and narrow diameter distribution. The average diameter, diameter distribution, tensile strength and crystallization of PCL–
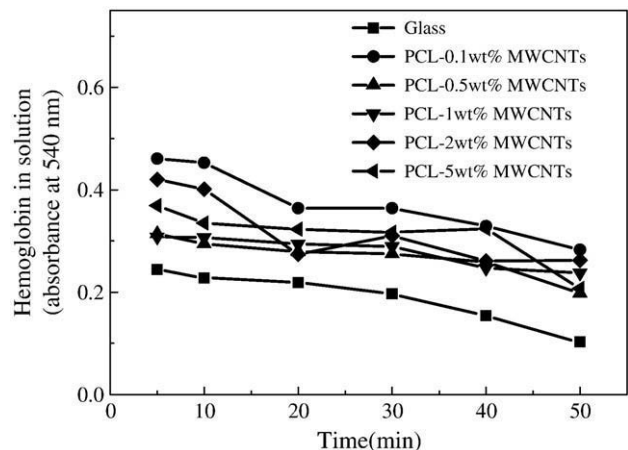
Fig. 8. Dynamic clotting time of electrospun PCL–MWCNTs nanofiber membranes.

MWCNTs nanofiber membranes increased with increasing amounts of MWCNTs filling content and then decreased due to further increasing the MWCNTs content. Moreover, the electrospun PCL/MWCNTs nanofiber membranes possessed good degradation, biocompatibility and hemocompatibility and have promising potentials in scaffold applications.

Acknowledgement

References

[1] D. Li, Y.N. Xia, Adv. Mater. 16 (2004) 1151.
[2] D.H. Reneker, I. Chun, Nanotechnology 7 (1996) 216.
[3] T.J. Sill, H.A. von Recum, Biomaterials 29 (2008) 1989.
[4] A. Bianco, E.D. Federico, I. Moscatelli, A. Camaioni, I. Armentano, L. Campagnolo, M. Dottori, J.M. Kenny, G. Siracusa, G. Gusmano, Mater. Sci. Eng. C 29 (2009) 2063.
[5] M. Ignatova, N. Manolova, I. Rashkow, Eur. Polym. J. 43 (2007) 1609.
[6] C.M. Vaz, S. van Tuijl, C.V.C. Bouten, F.P.T. Baaijens, Acta Biomater. 1 (2005) 575.
[7] O. Suwantong, P. Opanasopit, U. Ruktanonchai, P. Supaphol, Polymer 48 (2007) 7546.
[8] H. Cho, J. An, Biomaterials 27 (2006) 544.
[9] Z. Cheng, S. Teoh, Biomaterials 25 (2004) 1991.
[10] E.J. Chong, T.T. Phan, I.J. Lim, Y.Z. Zhang, B.H. Bay, S. Ramakrishna, C.T. Lim, Acta Biomater. 3 (2007) 321.
[11] Y. Duan, J. Jia, S. Wang, W. Yan, L. Jin, Z. Wang, J. Appl. Polym. Sci. 106 (2007) 1208.
[12] G.R. Patzke, F. Krumeich, R. Nesper, Angew. Chem. Int. Ed. 41 (2002) 2446.
[13] Y. Xia, P. Yang, Y. Sun, Y. Wu, B. Mayers, B. Gates, Y. Yin, F. Kim, H. Yan, Adv. Mater. 15 (2003) 353.
[14] S. Iijima, Nature 354 (1991) 56.
[15] P.M. Ajayan, Chem. Rev. 99 (1999) 1787.
[16] J. Thomassin, X. Lou, C. Pagnoulle, A. Saib, L. Bednarz, I. Huynen, R. Jerome, C. Detrembleur, J. Phys. Chem. C 111 (2007) 11186.
[17] D. Zhang, M.A. Kandadai, J. Cech, S. Roth, S.A. Curran, J. Phys. Chem. B 110 (2006) 12910.
[18] X. Zhang, J. Zhang, Z. Liu, Carbon 43 (2005) 2186.
[19] G.X. Chen, Y.J. Li, H. Shimizu, Carbon 45 (2007) 2334.
[20] L. Shao, Y.P. Bai, X. Huang, L.H. Meng, J. Ma, J. Appl. Polym. Sci. 113 (2009) 1879.
[21] Y. Zeng, Z. Ying, J.H. Du, H.M. Cheng, J. Phys. Chem. C 111 (2007) 13945.
[22] G. Wang, Z.K. Tan, X.Q. Liu, S. Chawda, J.S. Koo, V. Samuilov, M. Dudley, Nanotechnology 17 (2006) 5829.
[23] K. Saeed, S.Y. Park, H.J. Lee, J.B. Baek, W.S. Huh, Polymer 47 (2006) 8019.
[24] V. Crescenzi, G. Manzini, G. Calzolari, C. Borri, Eur. Polym. J. 8 (1972) 449.
[25] Y. Imai, Y. Nose, J. Biomed. Mater. Res. 6 (1972) 165.
[26] C. Meechaisue, R. Dubin, P. Supaphol, V.P. Hoven, J. Kohn, J. Biomater. Sci. Polym. Ed. 17 (2006) 1039.
[27] J.H. Sung, H.S. Kim, H.J. Jin, H.J. Choi, I.J. Chin, Macromolecules 37 (2004) 9899.
[28] K.H. Lee, H.Y. Kim, M.S. Khil, Y.M. Ra, D.R. Lee, Polymer 44 (2003) 1287.
[29] M.V. Jose, B.W. Steinert, V. Thomas, D.R. Dean, M.A. Abdalla, G. Price, G.M. Janowski, Polymer 48 (2007) 1069.
[30] X.Y. Huang, P.K. Jiang, C. Kim, F. Liu, Y. Yin, Eur. Polym. J. 45 (2009) 377.
[31] H. Uehara, K. Kato, M. Kakiage, T. Yamanobe, T. Komoto, J. Phys. Chem. C 111 (2007) 18950.
[32] L. Li, C.Y. Li, C. Ni, J. Am. Chem. Soc. 128 (2006) 1692.
[33] M. Moniruzzaman, J. Chattopadhyay, W.E. Billups, K.I. Winey, Nano Lett. 7 (2007) 1178.
[34] L. Li, L.M. Bellan, H.G. Craighead, M.W. Frey, Polymer 47 (2006) 6208.
[35] K. Rezwan, Q.Z. Chen, J.J. Blaker, A.R. Boccaccini, Biomaterials 27 (2006) 3413.
[36] W.J. Li, J.A. Cooper Jr, R.L. Mauck, R.S. Tuan, Acta Biomater. 2 (2006) 377.
[37] M.A. Correa-Duarte, N. Wagner, J. Rojas-Chapana, C. Morsczeck, M. Thie, M. Giersig, Nano Lett. 4 (2004) 2233.
[38] L.P. Zanello, B. Zhao, H. Hu, R.C. Haddon, Nano Lett. 6 (2006) 562.
[39] S. Kang, M. Herzberg, D.F. Rodrigues, M. Elimelech, Langmuir 24 (2008) 6409.
[40] A. Shvedova, V. Castranova, E. Kisin, D. Schwegler-Berry, A. Murray, V. Gandelsman, A. Maynard, P. Baron, J. Toxicol. Environ. Heal. A 66 (2003) 1909.
[41] J.M. Worle-Knirsch, K. Pulskamp, H.F. Krug, Nano Lett. 6 (2006) 1261.
[42] Chinese National Standard for Medical Devices and Implants-GB/T 16175-1996, 2003, pp. 6–8.
[43] R.K. Dey, A.R. Ray, Biomaterials 24 (2003) 2985.